
Learning Inverse Mappings with Adversarial Criterion

Jiyi Zhang¹ Hung Dang¹ Hwee Kuan Lee² Ee-Chien Chang¹

Abstract

We propose a flipped-Adversarial AutoEncoder (F-AAE) that simultaneously trains a generative model G that maps an arbitrary latent code distribution to a data distribution and an encoder E that embodies an “inverse mapping” that encodes a data sample into a latent code vector. Unlike previous hybrid approaches that leverage adversarial training criterion in constructing autoencoders, F-AAE minimizes re-encoding errors in the latent space and exploit adversarial criterion in the data space. Experimental evaluations demonstrate that the proposed frameworks produces sharper reconstructed image t and while at the same time enabling inference that captures rich semantic representation of data.

1. Introduction

Learning *generative* models that capture the rich semantic representation of data has been long considered a key challenge in the field of machine learning (Chang et al., 2008). Generative models, or *generators* for short, are tasked to learn structured probability distributions, specifying a hypothetical casual process by which data are to be generated from latent structure (Griffiths et al., 2007). In another words, a generator maps an arbitrary latent code distribution to the data distribution, and has to be learned from a sparse training set. Early approaches to construct generative models were typically based on maximum likelihood estimation, requiring approximating many intractable probabilistic computations (Salakhutdinov & Larochelle, 2010). More recently, Goodfellow et al. proposed Generative Adversarial Networks (GAN) as an alternative technique to learn generative models (Goodfellow et al., 2014), embodying an adversarial training criterion so as to sidesteps difficulties faced by earlier approach. More specifically, the generator is pitted against a *discriminative* model (a.k.a. *discrimina-*

tor) which attempts to discriminate samples drawn from the training data, from data generated by generator. The GAN framework has been empirically shown to obtain impressive results on natural images (Radford et al., 2015; Denton et al., 2015).

Beside the generator, there are also strong interests in its inverse, that is, encoder that maps the data distribution to the latent code distribution. Such a pair of generator and encoder would enable a wider range of applications, for instances, feature representation, noise removal via reconstruction, etc. An autoencoder, in contrast to GAN, learns both generator and encoder simultaneously and there are extensive work on autoencoder construction (Kingma & Welling, 2013). In view of the effectiveness of GAN, many have considered leveraging adversarial training criterion to learn the encoder, notably Adversarial AutoEncoder (AAE) (Makhzani et al., 2015) and BiGAN (Donahue et al., 2016). While these frameworks provide mechanisms to simultaneously train a pair of generator (or a decoder in AAE’s terminology) and encoder altogether, thus addressing the problem at hand to some extent, each has its own limitations. In particular, images generated by AAE tend to be overly “smoothed”, while those generated by BiGAN, although appear sharper, often vaguely resemble the original images.

In this paper, we propose *flipped-Adversarial AutoEncoder* (F-AAE). Our framework is inspired by AAE (Makhzani et al., 2015). Nevertheless, we introduce subtle yet significant modifications: flipping the positions of the encoder E_ϕ and generator G_θ in the training pipeline, and operating the discriminator D_w in data space. Figure 1 depicts the architecture of our proposed framework. F-AAE feeds a latent code vector \mathbf{z} drawn from a prior distribution $p_z(\mathbf{z})$ into the generator G_θ and sample \mathbf{x} drawn from the data distribution $p_x(\mathbf{x})$ into the discriminator D_w . The output $\hat{\mathbf{x}}$ of G_θ is then pipelined to E_ϕ , which re-encodes $\hat{\mathbf{x}}$ back into a latent code vector $\hat{\mathbf{z}}$. The generated image $\hat{\mathbf{x}}$ is also fed into D_w , which attempts to discriminate $\hat{\mathbf{x}}$ from \mathbf{x} .

While F-AAE is similar to AAE in the use of dual objectives of an *error criterion* and an *adversarial criterion*, the above-mentioned flipping leads to two key differences. Firstly, our framework measures and attempts to minimize the error (which we called *re-encoding error*) in the latent space,

¹School of Computing, National University of Singapore. ²Bioinformatic Institute, Agency for Science, Technology and Research. Correspondence to: Hung Dang <hungdang@comp.nus.edu.sg>.

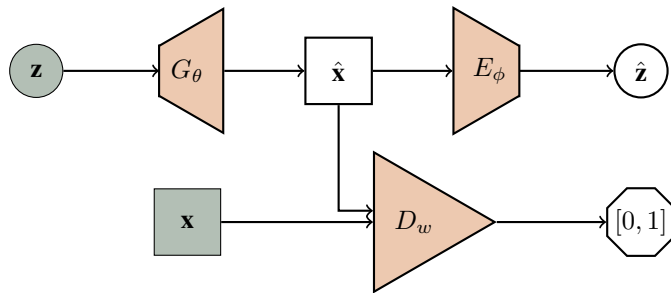


Figure 1. The proposed F-AAE framework. A latent code vector $\mathbf{z} \sim p_z(\mathbf{z})$ is fed into the generator G_θ , while an image $\mathbf{x} \sim p_x(\mathbf{x})$ is fed into the discriminator D_w . The output $\hat{\mathbf{x}}$ of G_θ is pipelined to E_ϕ , which re-encodes $\hat{\mathbf{x}}$ into a latent code vector $\hat{\mathbf{z}}$. The generated image $\hat{\mathbf{x}}$ is also fed into D_w , which attempts to discriminate $\hat{\mathbf{x}}$ from \mathbf{x} .

as opposed to AAE minimizing the *reconstruction error* between real and reconstructed images measured in the data space under some distance function (e.g. ℓ_2 norm). The rationale of focusing on re-encoding error is that, latent space arguably carries semantic information. As such, optimising the error in latent space would minimise perturbation of semantic representation of data. Secondly, the discriminator D_w in our framework operates in the data space, as opposed to that of AAE operating in the latent space. This adversarial learning criterion enables F-AAE to train the generator G_θ to produce samples as close to the data distribution p_x as possible, overcoming the “smoothing” effect of AAE.

Our experimental evaluations demonstrate the advantages F-AAE has over AAE and BiGAN. Figure 7 shows the reconstructed images produced by AAE, BiGAN and F-AAE, respectively, on the ImageNet dataset. We observe that F-AAE tends to produce sharper images compared to AAE, supporting the rationale of operating the discriminator in the data space. We also find that the images generated by F-AAE visually resemble the original real images better than BiGAN’s reconstructions, suggesting that F-AAE attains generator and encoder that are closer to the inverse of each other. We suspect that this is because BiGAN, unlike AAE and F-AAE, does not explicitly minimise reconstruction error. Instead, the framework attempts to match two joint distributions in the data and latent space, which indirectly gives encoder and generator that are inverse of each other. However, in practice, it is arguably difficult to meet the matching condition, and in such sub-optimal situation, it is not clear whether the reconstruction error would be small, even if the two joint distributions are close.

In summary, our paper makes the following contributions:

1. We propose a novel framework, namely flipped-Adversarial AutoEncoder (F-AAE), to simultaneously train a generator G_θ , and an encoder E_ϕ considered as an “inverse” mapping of G_θ . F-AAE objective minimizes re-encoding errors in the latent space and exploits adversarial criterion in the data space.
2. We conduct intensive experiment studies on standard datasets to empirically demonstrate that F-AAE could produce high-quality samples, and at the same time enable inference that captures rich semantic representation of data.

2. Background

2.1. Notations

Let us first introduce some common variables and operators. Variables include latent code vectors $\mathbf{z} \in \mathbb{R}^n$ sampled from a known distribution $p_z(\mathbf{z})$, generated latent code vectors $\hat{\mathbf{z}} \in \mathbb{R}^n$, data points $\mathbf{x} \in \mathbb{R}^d$ drawn from the prior data distribution $p_x(\mathbf{x})$ and generated data points $\hat{\mathbf{x}} \in \mathbb{R}^d$. When it is clear from the context, we abuse the notation, denoting $p_z(\mathbf{z})$ by p_z and $p_x(\mathbf{x})$ by p_x .

The operators include the *generator* (a.k.a. *decoder*) $G_\theta : \mathbb{R}^n \mapsto \mathbb{R}^d$, the *encoder* $E_\phi : \mathbb{R}^d \mapsto \mathbb{R}^n$ and the *discriminator* D_w . The generator G_θ takes as input either \mathbf{z} or $\hat{\mathbf{z}}$, and outputs a generated data point $\hat{\mathbf{x}}$. Thus, it plays a similar role to that of a generative network in the original GANs (Goodfellow et al., 2014). The encoder E_ϕ takes as input either a real data point \mathbf{x} or a generated data point $\hat{\mathbf{x}}$, and outputs an encoded latent vector $\hat{\mathbf{z}}$. Finally, the discriminator D_w takes in a pair of inputs, and is tasked to discriminate one from another. There are different functional forms of discriminator in different frameworks, which we shall elaborate in respective sections. The operators in this paper are all neural networks parameterized by θ, ϕ, w for the generator, encoder and discriminator, respectively.

2.2. GAN

The GAN framework defines a min-max adversarial game which pits a generative model G_θ against a discriminative model D_w , as depicted in Figure 2. The generator G_θ maps a latent code vector $\mathbf{z} \sim p_z(\mathbf{z})$, generating a sample $\hat{\mathbf{x}}$. At the same time, the discriminator D_w evaluates the probability that a given sample \mathbf{x} is drawn from the true data

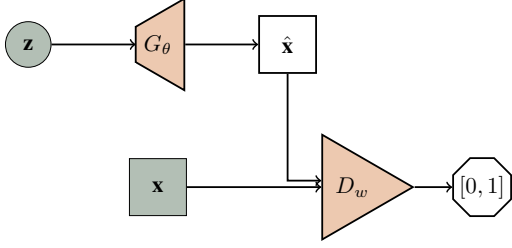


Figure 2. GAN Framework. Unlike F-AAE, GAN only consists of G_θ and D_w . It lacks an encoder E_ϕ that maps a generated sample $\hat{\mathbf{x}}$ into an encoded latent code vector $\hat{\mathbf{z}}$, which can essentially serves as an inverse of G_θ .

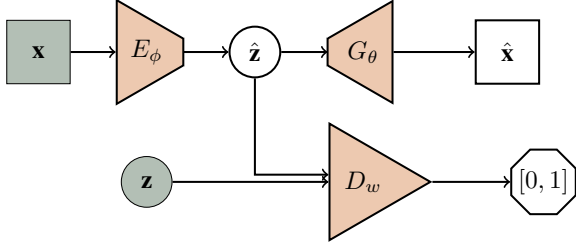


Figure 3. AAE framework. In contrast to F-AAE, AAE feeds real data samples drawn from the data distribution $p_x(\mathbf{x})$ into E_ϕ , and exploits D_w to impose a certain properties on encoded latent vector $\hat{\mathbf{z}}$ that are generated by E_ϕ .

distribution $p_x(\mathbf{x})$, instead of the generated by G_θ . The optimal solution for this adversarial game is a pair of G_θ and D_w that optimizes the following function (Goodfellow et al., 2014):

$$\min_{\theta} \max_w \mathcal{A}(G_\theta, D_w) \quad \text{where} \quad (1)$$

$$\mathcal{A}(G_\theta, D_w) = \mathbb{E}_{\mathbf{x} \sim p_x} [\log D_w(x)] + \mathbb{E}_{\mathbf{z} \sim p_z} [\log(1 - D_w(G_\theta(z)))]$$

As mentioned in the previous section, GAN does not directly provide the encoder, that is, the inverse of the generator G_θ . Although one may apply generic method to invert the generator G_θ produced by GAN, however, it is not clear how to accurately and efficiently compute such inverse. Moreover, even if the inverse can be accurately derived from G , the inverse mapping might not be continuous and smooth, and thus does not give a meaningful encoding that captures data semantic.

2.3. Adversarial AutoEncoders

Adversarial AutoEncoder (Makhzani et al., 2015) (AAE) framework introduces an additional constraint into the classical variational autoencoder (VAE) (Kingma & Welling, 2013) so as to enforce the “hidden” latent code of the autoencoder to observe statistical properties of some given prior

distribution, thus guarantees that the hidden latent code generated from any part of the data space would result in meaningful samples. More specifically, while VAE make leverages KL divergence penalty to impose a prior distribution on the hidden latent code of the autoencoder, AAE employs an adversarial training to match the aggregated posterior with the prior distribution. The adversarial training procedure, similar in spirit to GAN, introduces a discriminative network $D_w : \mathbb{R}^n \mapsto \mathbb{R}$ into the training pipeline of the autoencoder. Note that unlike in the case of GAN, the discriminator for AAE maps the latent vector \mathbf{z} or $\hat{\mathbf{z}}$ into the discriminator score. D_w is trained to distinguish a latent code generated by the autoencoder from a real sample drawn from the prior distribution. The encoder is then trained to maximally confused D_w , while at the same time, optimized to minimize the reconstruction error of the autoencoder.

From a prior distribution p_z , the data distribution p_x and some distance function $d(\cdot, \cdot)$, AAE jointly trains all three networks G_θ , E_ϕ and D_w by optimizing the following objective function (Figure 3):

$$\min_{\theta, \phi} \max_w \mathcal{B}(G_\theta, E_\phi, D_w) \quad \text{where} \quad (2)$$

$$\mathcal{B}(G_\theta, E_\phi, D_w) = \mathbb{E}_{\mathbf{z} \sim p_z} [\log D_w(\mathbf{z})] + \mathbb{E}_{\mathbf{x} \sim p_x} [\log(1 - D_w(E_\phi(\mathbf{x})))] + \mathbb{E}_{\mathbf{x} \sim p_x} [d(\mathbf{x}, G_\theta(E_\phi(\mathbf{x})))]$$

The first two terms quantify the performance of the discriminator with respect to the encoder (that is, how well the prior distribution matches the aggregated posterior), and the last term is the *reconstruction error* incurred by the composition of encoder follows by generator. A typical choice of the distance function is ℓ_2 or ℓ_1 norm.

Note that in a solution with non-zero reconstruction error, the pair G_θ and E_ϕ are not the exact inverse of each other. Indeed empirically, when applying to images, the reconstructed error are small but nonetheless non-zero. Since the images within a bounded distance from the data are mostly smoothed images, we would expect overly smoothed reconstructed images, as depicted in Figure 5 and 6.

2.4. BiGan

BiGAN takes an interesting approach in learning the encoder. The discriminator attempts to discriminate joint distributions in the data and latent space, that is, discriminating $(G_\theta(\mathbf{z}), \mathbf{z})$ verse $(\mathbf{x}, E_\phi(\mathbf{x}))$. The adversarial game optimises the following function:

$$\min_{\theta, \phi} \max_w \mathcal{C}(G_\theta, E_\phi, D_w) \quad \text{where} \quad (3)$$

$$\mathcal{C}(G_\theta, E_\phi, D_w) = \mathbb{E}_{\mathbf{x} \sim p_{data}} [\log D_w(E_\phi(x), x)] + \mathbb{E}_{\mathbf{z} \sim p_z} [\log(1 - D_w(z, G_\theta(z)))]$$

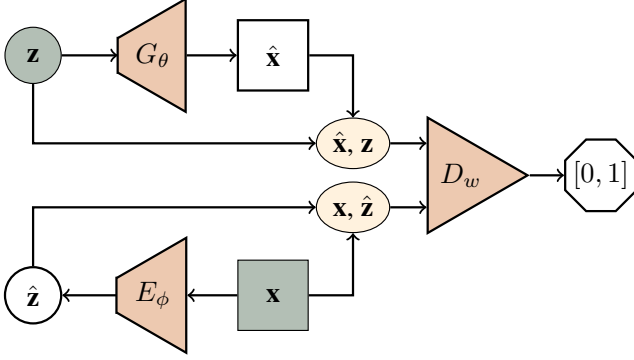


Figure 4. BiGAN framework. As opposed to the F-AAE discriminator, the discriminator of BiGAN receives joint pairs of latent code vector and data sample. In addition, BiGAN objective functions does not explicitly minimize reconstruction error.

Although there is no explicit reconstruction loss term in the objective function, it can be shown that with the optimal encoder E_{ϕ^*} and generator G_{θ^*} , the two joint distributions match, which in turn implies E_{ϕ^*} is the inverse of the G_{θ^*} almost everywhere (Donahue et al., 2016). However, in practice it is challenging to achieve optimality, and unfortunately, it is not clear whether the reconstruction error would be small at near-optimal. Empirically, for images, $G_{\theta}(E_{\phi}(x))$ is visually far from x , as depicted in Figure 5 and 6.

3. Flipped Adversarial Auto Encoder (F-AAE)

In this section, we present Flipped Adversarial Auto Encoder (F-AAE), contrasting our proposed framework against BiGAN, AAE, and Latent Vector Recovery.

3.1. Frame of F-AAE

The inputs of F-AAE training processes comprise latent vectors $\mathbf{z} \in \mathbb{R}^n$ from a known distribution $p_z(\mathbf{z})$ and samples from the data distribution $p_x(\mathbf{x})$. Associated operators are the generator G_{θ} , the encoder E_{ϕ} and the discriminators D_w whose functions were explained in the previous section.

Our framework jointly trains all three networks G_{θ} , E_{ϕ} and D_w by optimizing the following objective function:

$$\min_{\theta, \phi} \max_w \mathcal{F}(G_{\theta}, E_{\phi}, D_w) \quad \text{where} \quad (4)$$

$$\mathcal{F}(G_{\theta}, E_{\phi}, D_w) = \mathbb{E}_{\mathbf{x} \sim p_x} [\log D_w(\mathbf{x})] + \mathbb{E}_{\mathbf{z} \sim p_z} [\log(1 - D_w(G_{\theta}(\mathbf{z})))] + \alpha \mathbb{E}_{\mathbf{z} \sim p_z} [\|\mathbf{z} - E_{\phi}(G_{\theta}(\mathbf{z}))\|]$$

The last term measures the difference after a latent vector \mathbf{z} is being “re-encoded”. While our objective function adopts

ℓ_2 norm, other distance functions are also applicable. The pre-defined constant α serves as a normalizing factor for the distance function. There are many options for the latent vector distribution $p_z(\mathbf{z})$. In our experiments, we sample the latent vector $\mathbf{z} \sim p_z(\mathbf{z})$ uniformly from a n dimensional unit sphere S^n ; i.e., a multivariate normal distribution conditioned on unit norm.

The training iterates two phases, namely *re-encoding* and *regularization*:

- Re-encoding phase: G_{θ} and E_{ϕ} are updated so as to minimize the re-encoding error between the input \mathbf{z} and the re-encoded latent vector $\hat{\mathbf{z}} = E_{\phi}(G_{\theta}(\mathbf{z}))$.
- Regularization phase: D_w is first updated to discriminate the real sample $\mathbf{x} \sim p_x(\mathbf{x})$ from the generated sample $\hat{\mathbf{x}} = G_{\theta}(\mathbf{z})$. Next, the generator G_{θ} is updated so as to maximally confuse the discriminator D_w .

At the end of a successful training, we obtain a generator G_{θ} that is capable of generating meaningful samples resembling those that are drawn from the true data distribution. In addition, we also obtain an encoder E_{ϕ} that approximates the inverse of G_{θ} such that the re-encoding error is small.

3.2. Architecture of D_w , G_{θ} and E_{ϕ}

The generator G_{θ} is a deconvolutional neural network which takes as input a vector from latent space. In our experiments, we represent such latent vector by a random array of dimension 256 sampled uniformly from a n -dimensional unit sphere. The output of G_{θ} has the same shape as the real sample training data; i.e., $32 \times 32 \times 3$ for CIFAR-10 and CelebA dataset, and $64 \times 64 \times 3$ for ImageNet dataset.

Up-sampling layers are interleaved with convolution layers to reshape the input latent vector and scale it to the same dimension as training data. Batch Normalization (Ioffe & Szegedy, 2015) is used in between the layers to reduce co-variate shift. A leaky ReLU layer is used after each Batch Normalization layer. The last layer uses a sigmoid function as the activation function to ensure the pixel value fall between 0 and 1 which is the same as our preprocessed and normalized dataset.

The encoder E_{ϕ} uses an almost identical architecture as the generator but in a reverse order. The up-sampling layers are replaced with max-pooling layers. As the end of the network, the feature map is flattened back to an array of the given latent dimension. The output shape of the encoder is the same as the input shape of the generator G_{θ} and the input shape of the encoder is the same as the output shape of the generator G_{θ} .

The discriminator D_w is also a convolutional neural network. The input shape is the same as the output shape of the

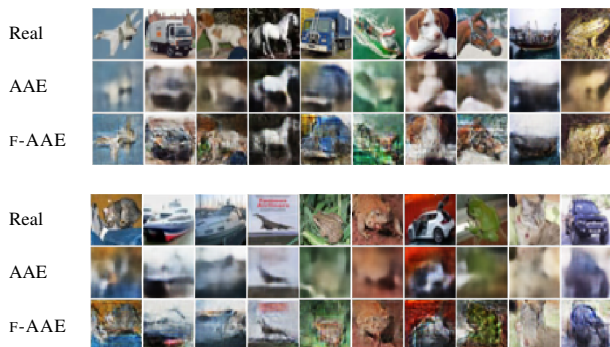


Figure 5. Reconstruction comparison between AAE and F-AAE on CIFAR-10 dataset using an image resolution of 32x32.

generator G_θ . The output is a probability indicating how real the input is. Sigmoid function is used as the activation function for the last layer to ensure the output falls between 0 and 1.

3.3. Relationship to Latent Vector Recovery

There are other ways to implement a reverse mapping of Generative Adversarial Network (GAN) (Goodfellow et al., 2014). Lipton & Tripathi et al. suggested the use of stochastic clipping which is a gradient-based technique to find the reverse function of an existing trained GAN generator (Lipton & Tripathi, 2017). F-AAE, in contrast, does not attempt to reverse arbitrary function. Instead, our framework provides a method to constrain the training of the generator, guaranteeing the existence of an approximate inverse mapping of the generator at any time during the training.

3.4. Relationship to Adversarial Autoencoder

F-AAE introduces a subtle yet significant modification over AAE’s architecture, which is to flip the positions of E_ϕ and G_θ in the training pipeline, and operating D_w in data space (Figure 1). This leads to two key differences. Firstly, F-AAE measures and minimizes the re-encoding error in the latent space, as opposed to AAE minimizing reconstruction error in data space. The phenomenon of vector arithmetic on the latent vectors in GAN suggest that imposing measurement on the latent vectors can yield meaningful results (Li & Luo, 2017). Secondly, operating D_w in the data space allows F-AAE to capture the data distribution $p_x(\mathbf{x})$ directly via the adversarial criterion. These advantage enables F-AAE the generator G_θ produce sharper images compared to that of AAE.

4. Empirical Evaluation

We present three use cases of F-AAE and benchmark it against AAE and BiGAN, which are the most related approaches to our work. BiGAN presents an interesting alter-



Figure 6. Reconstruction comparison between AAE and F-AAE on CelebA dataset using an image resolution of 32x32.

native method of finding the inverse of image generation without explicitly calculating re-encoding or reconstruction loss. Comparison are performed on the three standard datasets which are CIFAR-10, ImageNet and CelebA. To enable reproducibility of our experiment results, we made a prototype of F-AAE available online¹.

4.1. Experiment Setup

We used CIFAR-10, CelebA and ImageNet datasets for our training and testing. The CIFAR-10 contains 50K training samples and 10K testing samples. Each image has a shape of $32 \times 32 \times 3$. The CelebA dataset comprises 202599 cropped and aligned face images. We resized the images to $32 \times 32 \times 3$, using five sixth of them for training and one sixth for testing. For ImageNet, we use the same dataset as Donahue et al. (Donahue et al., 2016), resizing the images to $64 \times 64 \times 3$. Our experiments normalize all the images so that each pixel takes a value in range $[0, 1]$.

For the comparison with AAE on CIFAR-10 and CelebA, we trained both F-AAE and AAE for 50 epoches. We set the same weightage of reconstruction/re-encoding loss and adversarial loss: 10^2 for reconstruction/re-encoding loss and 0.1 for adversarial loss. We used Adam optimizer and the same learning rate for F-AAE and AAE: $3 \cdot 10^{-4}$ for generator and 10^{-3} for discriminator. We also use the same decay rate for these two models: 10^{-4} for both generator and discriminator.

Since we were not able to reproduce the BiGAN results, we restrict the benchmark against BiGAN to ImageNet dataset, taking the results from BiGAN paper directly and presenting them in Figure 7. In this set of experiments, we trained F-AAE and AAE for 600 epoches, using the same optimizer, learning rate and decay rate as above. For the weightage of reconstruction/re-encoding loss and adversarial loss, we used 30 for reconstruction/re-encoding loss and 0.1 for adversarial loss in the first 200 epoches and 100 for

¹<https://github.com/zhangjiyi/FAAE>

Learning Inverse Mappings with Adversarial Criterion

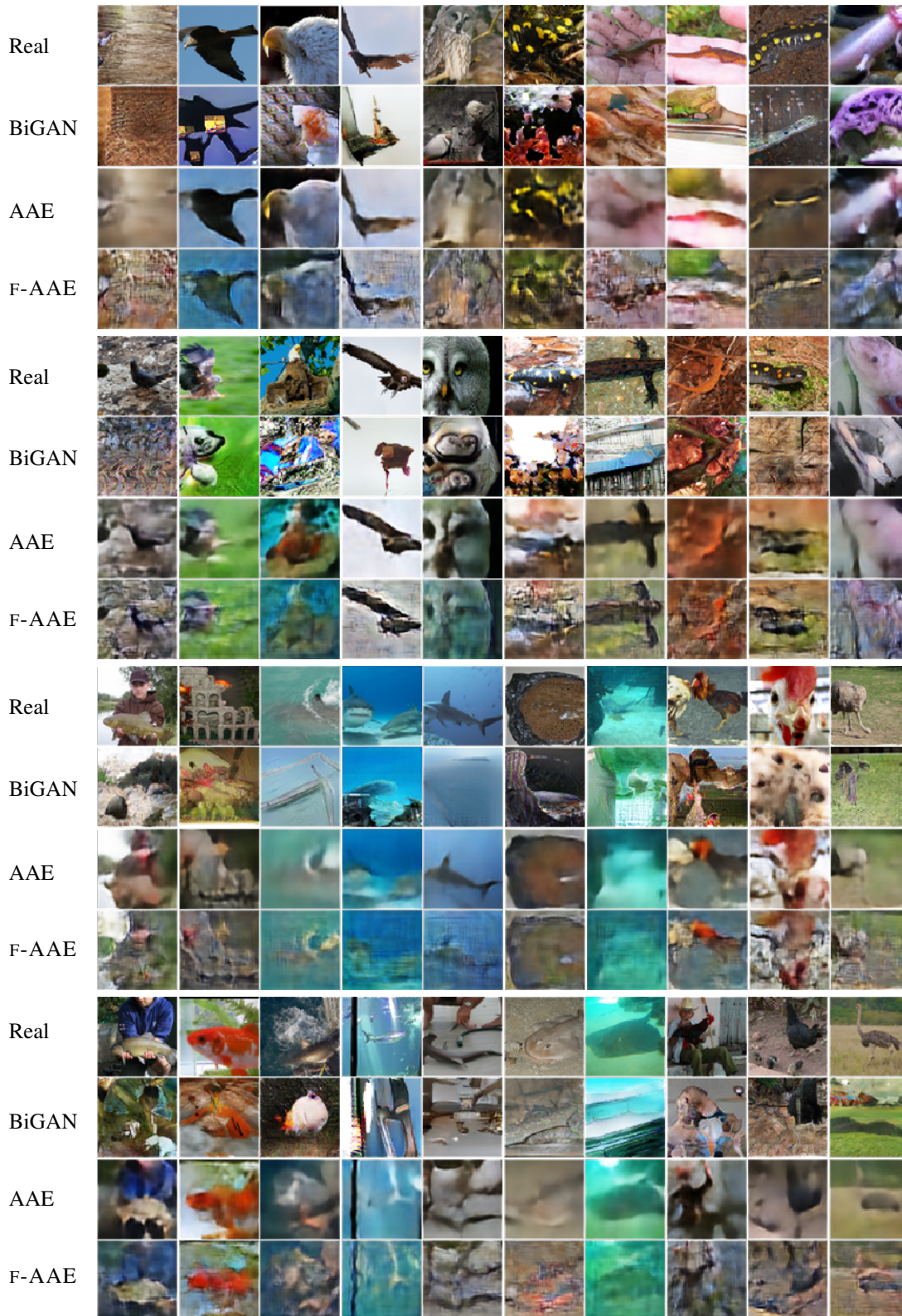


Figure 7. Reconstruction comparison between BiGAN, AAE and F-AAE on ImageNet dataset. BiGAN generally does not reconstruct well and AAE reconstructions are blurry. Images reconstructed using F-AAE contain some noise and artifacts.

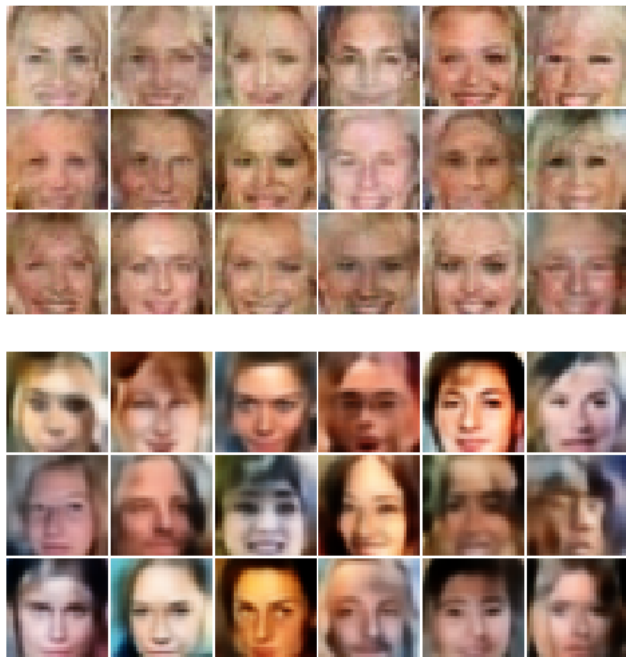


Figure 8. Randomly generated faces by F-AAE (top panel) and AAE (bottom panel) trained for image resolution of 32x32.

reconstruction/re-encoding loss and 0.1 for adversarial loss for the rest epoches. The training of AAE and F-AAE in our experiments always take the same parameters.

4.2. Image Reconstruction

The first comparison is done on the image reconstruction tasks wherein images are encoded into latent space representations and then reconstructed back into the data space. Figure 5 and 6 show reconstructions of CIFAR-10 images using AAE and F-AAE. AAE tends to produce blurry reconstructions whereas F-AAE produce sharper images.

Note that for the CelebA data set, a majority of the training images are frontal photos of the faces. Since F-AAE is trained based on re-encoding errors measured in the latent semantic space, F-AAE tends to reconstruct semantic representation, which is mostly frontal views for this dataset. That is, given a side view face photo, F-AAE has the tendency to “turn” the face into a frontal view. Some examples of this phenomenon is highlighted with arrows in Figure 6.

Figure 7 shows reconstruction results in comparison with BiGAN and AAE. We find that BiGAN observes numerous reconstruction failures. For example, the eagles in the top first and second panels, the owl in the second panel and birds in the third panel cannot be reconstructed. While it can be proven that BiGAN converges to inverse mappings, it is unclear if conditions for obtaining convergence to global minimum could be met in actual training.

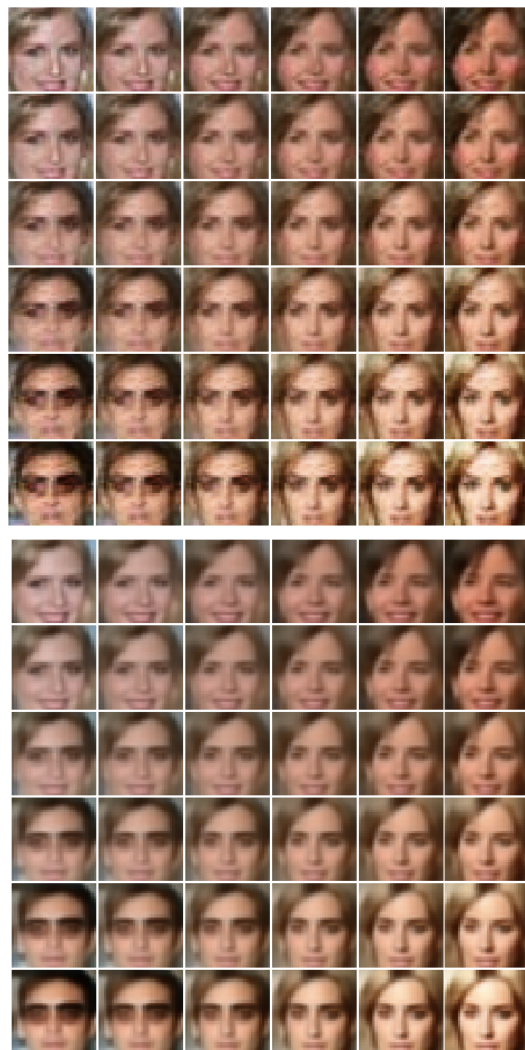


Figure 9. F-AAE (top) and AAE (bottom) results for image morphing. Images at the four corners of each panel are reconstructions of real images. The rest were generated from linear combinations of the latent space representations of the real images.

4.3. Image Generation

Random “meaningful” images can also be generated by feeding latent code vectors sampled in the latent space to the generator G_θ . Figure 8 depicts generated faces using the CelebA data set as the training set, with top panels are those produced by F-AAE while bottom panel is generated using AAE. As expected, we find that images generated using AAE tend to be blurry.

4.4. Image Morphing through vector arithmetic

With good generator and encoder that are inverses of each other, image morphing can be performed by mapping images into latent vectors, perturbing the latent vectors and

mapping them back onto the data space. Figure 9 demonstrate results of image morphing using F-AAE and AAE. The same experiments are performed for both methods. In the image panels, four corner images are generated by manually choosing four original images, encoding them into latent space and reconstructing the images from the encoded latent vectors. Let the (un-normalized) encoded latent vectors be $\mathbf{z}_1, \mathbf{z}_2, \mathbf{z}_3$ and \mathbf{z}_4 , our experiment generates their linear combinations as follow:

$$\mathbf{l} = \alpha_1 \mathbf{z}_1 + \alpha_2 \mathbf{z}_2 + \alpha_3 \mathbf{z}_3 + \alpha_4 \mathbf{z}_4 \quad (5)$$

We then normalize $\mathbf{z}' = \mathbf{l}$ to generate a new latent vector that will be a sample from p_z . Finally, we map \mathbf{z}' back into the data space, attaining \mathbf{x}' . By gradually varying α_i , this mechanism achieve an effect of morphing.

We plot the morphed images produced by F-AAE and AAE in Figure 9. We observe that images generated by AAE (bottom panel) are blurry and visually less consistent. For example, the images in the center of the AAE panel seems appears more smoothed than those at the corners. F-AAE generated images, on the other hand, are visually more consistent throughout the panel. We believe that this is by courtesy of operating F-AAE’s discriminator in the data space.

5. Related Work

The GAN framework has inspired a vast body of research in the literature, focusing on either augmenting GANs with additional functionality or improving its performance. Huang et al. explored a generative model which is used to invert hierarchical representations of a discriminative network (Huang et al., 2017). Mirza et al. presented conditional GAN (cGAN), augmenting GANs such that the data generation is conditioned by both intrinsic (i.e., latent code vector) and extrinsic (i.e., known auxiliary information) factors (Mirza & Osindero, 2014). Perarnau et al. and Jaiswal et al. discussed techniques for learning inverse mappings of generators pretrained under cGAN (Perarnau et al., 2016; Jaiswal et al., 2017). Our framework, on the other hand, focuses solely on learning the generator and its inverse mapping simultaneously, without constraining the data generation with any extrinsic factors or attempting to invert discriminative networks.

Other related proposals that focus on training both the generator and the encoder under the GAN framework include BiGAN (Donahue et al., 2016) and adversarially learned inference (ALI) model (Dumoulin et al., 2016). While F-AAE shares with these proposals the use of adversarial training criterion, our framework operates the discriminator in a different fashion. In particular, while the discriminators in BiGAN and ALI receive joint pairs of latent code vector and data sample (\mathbf{x}, \mathbf{z}) , the discriminator in F-AAE operates solely in the data space. Besides, BiGAN and ALI do not

explicitly minimizing reconstruction errors, as opposed to F-AAE does.

Perhaps most closely related to F-AAE is the Adversarial AutoEncoder (AAE) (Makhzani et al., 2015). AAE is an extension of the Variational Autoencoders (VAE) (Kingma & Welling, 2013), and thus suffering from VAE’s limitation wherein samples generated by the decoder are blurry and overly smoothed. F-AAE overcomes this limitation by pitting G against a discriminator D operating in the data space, thus enabling the generator G to produce samples as close to the data distribution p_x as possible (i.e., attaining higher visual quality). Another point contrasting AAE and F-AAE is a mechanism that encourages the encoder distribution to match with the prior distribution of the latent code vector. F-AAE attains this by imposing mean square error criterion on latent code vectors, instead of AAE’s use of the discriminator operating in the latent space.

6. Conclusion and Future Work

We have presented the flipped-Adversarial AutoEncoder that simultaneously trains a generative model G that maps arbitrary latent code distribution to the data distribution, and an encoder E that can be considered as an “inverse” mapping of G . The key technical novelty of F-AAE lies in its optimization strategy which minimizes re-encoding errors in the latent space and exploits adversarial criterion in the data space. We have empirically demonstrated on various standard datasets that F-AAE could produce high-quality samples, and at the same time enable inference that captures rich semantic representation of data.

The proposed F-AAE framework potentially enables a range of interesting applications. We hypothesize that a good pair of generator and decoder that allow bidirectional mapping between a complex data distribution and a simpler latent distribution can be used to learn underlying image manifold via differential latent vector arithmetic. In particular, given an image \mathbf{x} , one can employ F-AAE’s encoder to encode \mathbf{x} into \mathbf{z} . A small perturbation can then be applied to the latent vector \mathbf{z} , obtaining $\mathbf{z}' = \mathbf{z} + \Delta \mathbf{z}$ which can be mapped (by the generator G) back onto a morphed image \mathbf{x}' . Successive applications of such morphing can be applied to build a path of images that connects two images \mathbf{x}_1 and \mathbf{x}_2 . This ability to gradually morph/transform one sample into another wherein all the intermediate samples along the path are all “meaningful” potentially has multiple use-cases. For example, the length of this path can be use as a meaningful measure of image distance for image retrieval. In addition, morphing can also be used for data augmentation or adversarial attacks. We leave our future works as the study of applications of F-AAE in security and privacy aspects of machine learning, in particular membership inference and evasion attacks (Shokri et al., 2017; Dang et al., 2017).

References

- Chang, Ming-Wei, Ratinov, Lev-Arie, Roth, Dan, and Sriku-mar, Vivek. Importance of semantic representation: Data-less classification. In *AAAI*, volume 2, pp. 830–835, 2008.
- Dang, Hung, Huang, Yue, and Chang, Ee-Chien. Evading classifiers by morphing in the dark. In *Proceedings of the 2017 ACM SIGSAC Conference on Computer and Communications Security*, pp. 119–133. ACM, 2017.
- Denton, Emily L, Chintala, Soumith, Fergus, Rob, et al. Deep generative image models using a laplacian pyramid of adversarial networks. In *Advances in neural information processing systems*, pp. 1486–1494, 2015.
- Donahue, Jeff, Krähenbühl, Philipp, and Darrell, Trevor. Adversarial feature learning. *arXiv preprint arXiv:1605.09782*, 2016.
- Dumoulin, Vincent, Belghazi, Ishmael, Poole, Ben, Lamb, Alex, Arjovsky, Martin, Mastropietro, Olivier, and Courville, Aaron. Adversarially learned inference. *arXiv preprint arXiv:1606.00704*, 2016.
- Goodfellow, Ian, Pouget-Abadie, Jean, Mirza, Mehdi, Xu, Bing, Warde-Farley, David, Ozair, Sherjil, Courville, Aaron, and Bengio, Yoshua. Generative adversarial nets. In *Advances in neural information processing systems*, pp. 2672–2680, 2014.
- Griffiths, Thomas L, Steyvers, Mark, and Tenenbaum, Joshua B. Topics in semantic representation. *Psychological review*, 114(2):211, 2007.
- Huang, Xun, Li, Yixuan, Poursaeed, Omid, Hopcroft, John, and Belongie, Serge. Stacked generative adversarial networks. In *IEEE Conference on Computer Vision and Pattern Recognition (CVPR)*, volume 2, pp. 4, 2017.
- Ioffe, Sergey and Szegedy, Christian. Batch normalization: Accelerating deep network training by reducing internal covariate shift. In *International conference on machine learning*, pp. 448–456, 2015.
- Jaiswal, Ayush, AbdAlmageed, Wael, Wu, Yue, and Natarajan, Premkumar. Bidirectional conditional generative adversarial networks. *arXiv preprint arXiv:1711.07461*, 2017.
- Kingma, Diederik P and Welling, Max. Auto-encoding variational bayes. *arXiv preprint arXiv:1312.6114*, 2013.
- Li, Zhigang and Luo, Yupin. Generate identity-preserving faces by generative adversarial networks. *arXiv preprint arXiv:1706.03227*, 2017.
- Lipton, Zachary C and Tripathi, Subarna. Precise recovery of latent vectors from generative adversarial networks. *arXiv preprint arXiv:1702.04782*, 2017.
- Makhzani, Alireza, Shlens, Jonathon, Jaitly, Navdeep, Goodfellow, Ian, and Frey, Brendan. Adversarial autoencoders. *arXiv preprint arXiv:1511.05644*, 2015.
- Mirza, Mehdi and Osindero, Simon. Conditional generative adversarial nets. *arXiv preprint arXiv:1411.1784*, 2014.
- Perarnau, Guim, van de Weijer, Joost, Raducanu, Bogdan, and Álvarez, Jose M. Invertible conditional gans for image editing. *arXiv preprint arXiv:1611.06355*, 2016.
- Radford, Alec, Metz, Luke, and Chintala, Soumith. Un-supervised representation learning with deep convolutional generative adversarial networks. *arXiv preprint arXiv:1511.06434*, 2015.
- Salakhutdinov, Ruslan and Larochelle, Hugo. Efficient learning of deep boltzmann machines. In *Proceedings of the Thirteenth International Conference on Artificial Intelligence and Statistics*, pp. 693–700, 2010.
- Shokri, Reza, Stronati, Marco, Song, Congzheng, and Shmatikov, Vitaly. Membership inference attacks against machine learning models. In *Security and Privacy (SP), 2017 IEEE Symposium on*, pp. 3–18. IEEE, 2017.